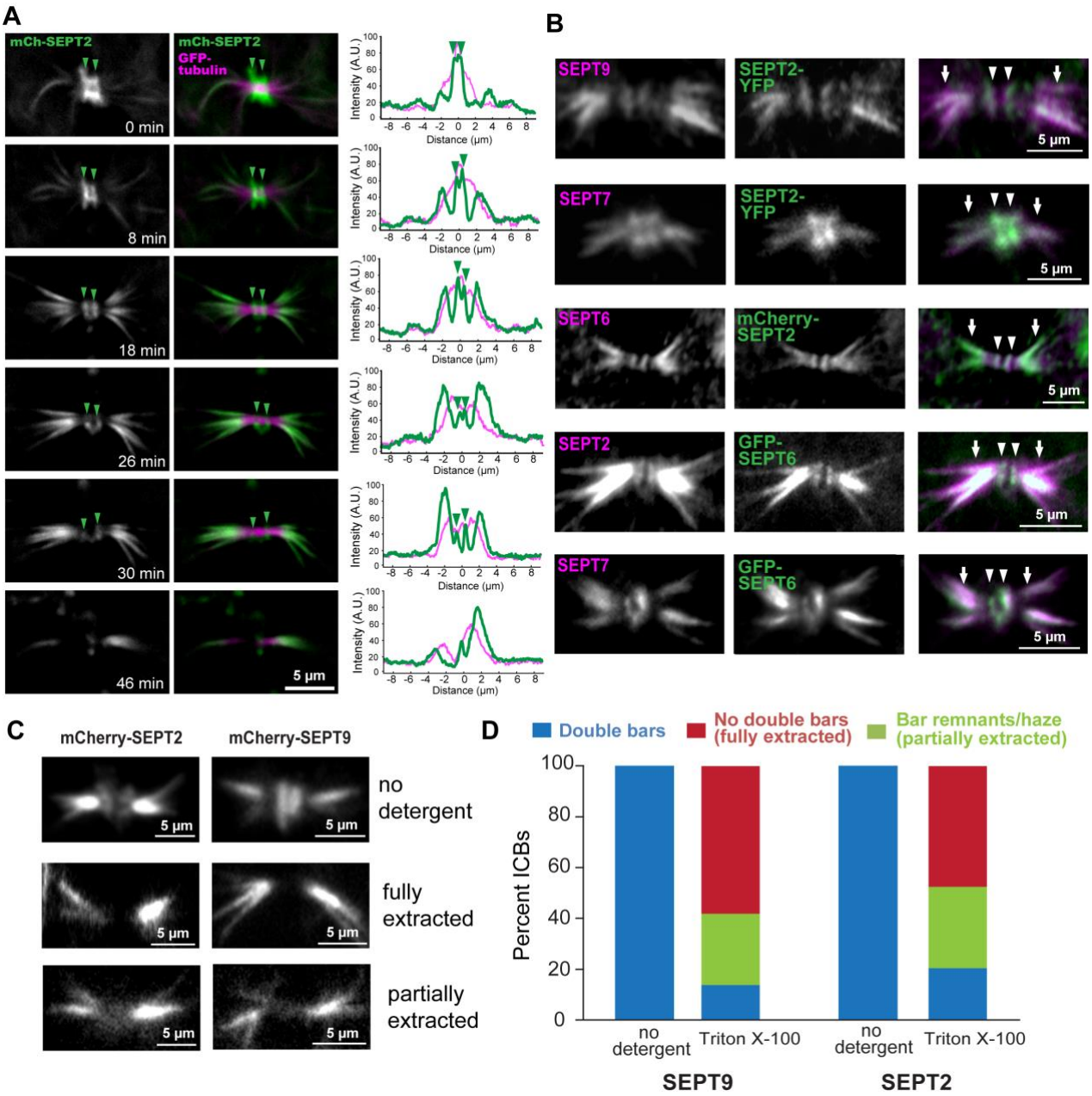

Figure S1. Septins 2, 6, 7 and 9 colocalize on distinct membrane and MT domains of the midbody. Related to Figure 1.

(A) Images show frames from time-lapse imaging of MDCK-mCherry-SEPT2 cells expressing GFP-α-tubulin. Arrowheads point to membrane-associated mCherry-SEPT2. Plots show a fluorescence line scan along nine microns left and right of the midbody center. See also Video S2.

(B) Stable MDCK cell lines that express SEPT2-YFP, mCherry-SEPT2 and GFP-SEPT6 were stained with antibodies against endogenous SEPT2, SEPT6, SEPT7 and SEPT9, and imaged by fluorescence microscopy. Arrowheads point to membrane-associated (see below) double bars and arrows point to MT segments of the ICB.

(C-D) Stable MDCK cell lines that express mCherry-SEPT2 and mCherry-SEPT9 were pre-extracted with Triton X-100 (0.1%) for 30 s prior to fixation and imaging. Representative images (C) show the ICBs of cells that were not pre-extracted (no detergent) and ICBs of cells, which were fully extracted (no septin double bars) or partially extracted, which resulted in a haze or remnants of septin fluorescence at the center of the midbody. Bar graphs (D) show quantification of ICBs (n = 52-60) of pre- and non-extracted cells after categorization of septin fluorescence at the center of the midbody into double bars, no double bars (fully extracted) or haze/remnants of the double bar (partially extracted). The analysis was restricted to ICBs with non-compacted MTs as the septin double bar dissipates in later stages of telophase when MTs become tightly compacted. Dramatic loss of septin double bars from the ICBs of pre-extracted cells indicates that the septin double bar is a membrane-associated structure.

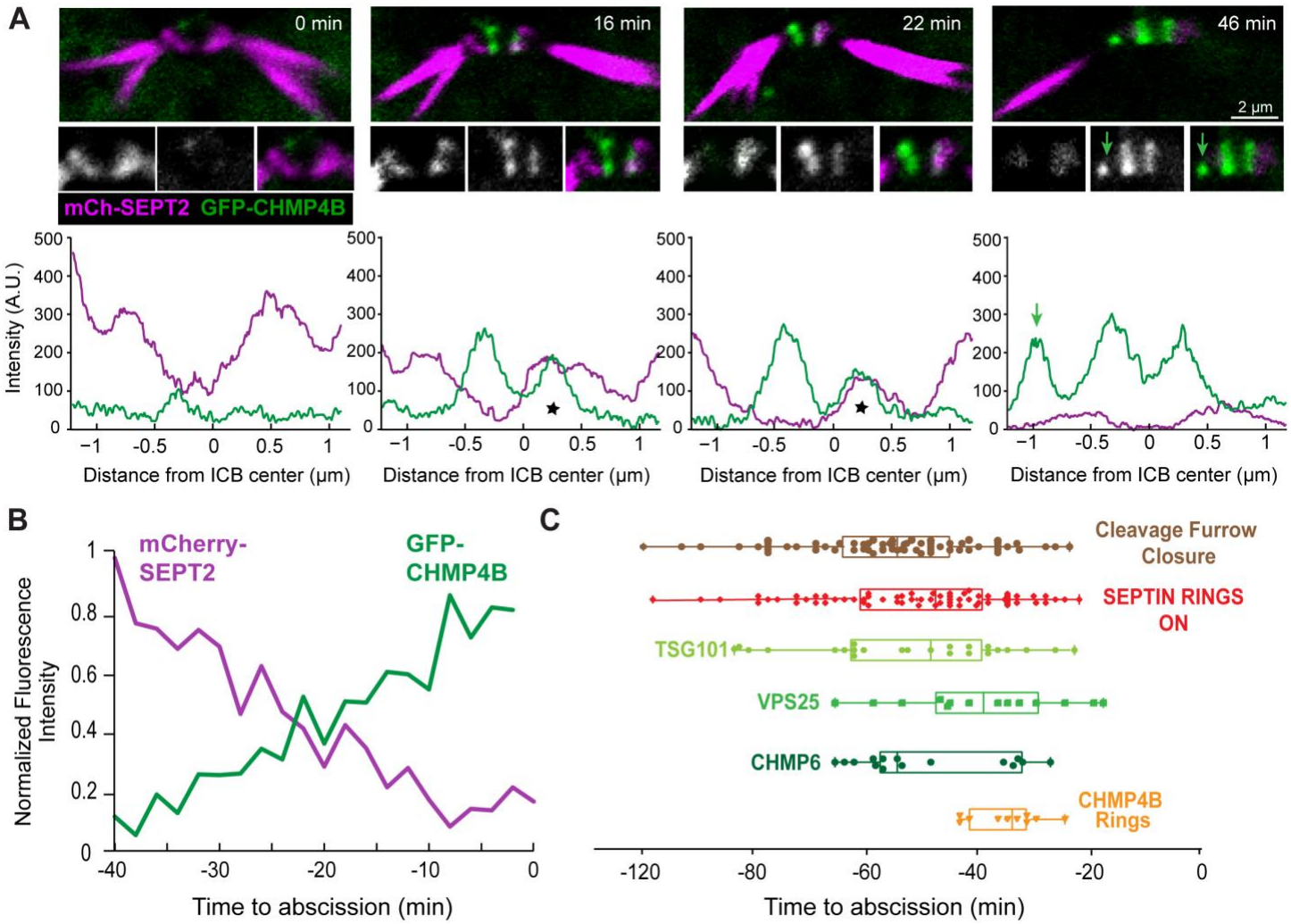

Figure S2. Spatiotemporal dynamics of SEPT2 with respect to ESCRT subunits. Related to Figure 2.

(A) Images show frames from movies of MCDK-mCherry-SEPT2 cells expressing GFP-CHMP4B. Plots show the mean pixel intensity of GFP-CHMP4B (green) across the width of the midbody. Asterisks highlight the overlap between SEPT2 and GFP-CHMP4B. Green arrow points to the lateral expansion of ESCRT-III into a cone.
(B) Plot shows the average fluorescence intensity of mCherry-SEPT2 and GFP-CHMP4B after normalization to a 0 (min intensity) to 1 (max intensity) range (n = 3 cells).
(C) Time-lapse microscopy movies of MDCK cells were analyzed to construct a temporal map of the timing of the cleavage furrow closure (n = 69), formation of septin rings (red; n = 71), which is denoted as septin rings "on", recruitment of GFP-TSG101 (n = 24), GFP-VPS25 (n = 15), CHMP6-GFP (n = 15) and CHMP4B-GFP (n = 11). All events were timed from the frame of ICB severing (t = 0).

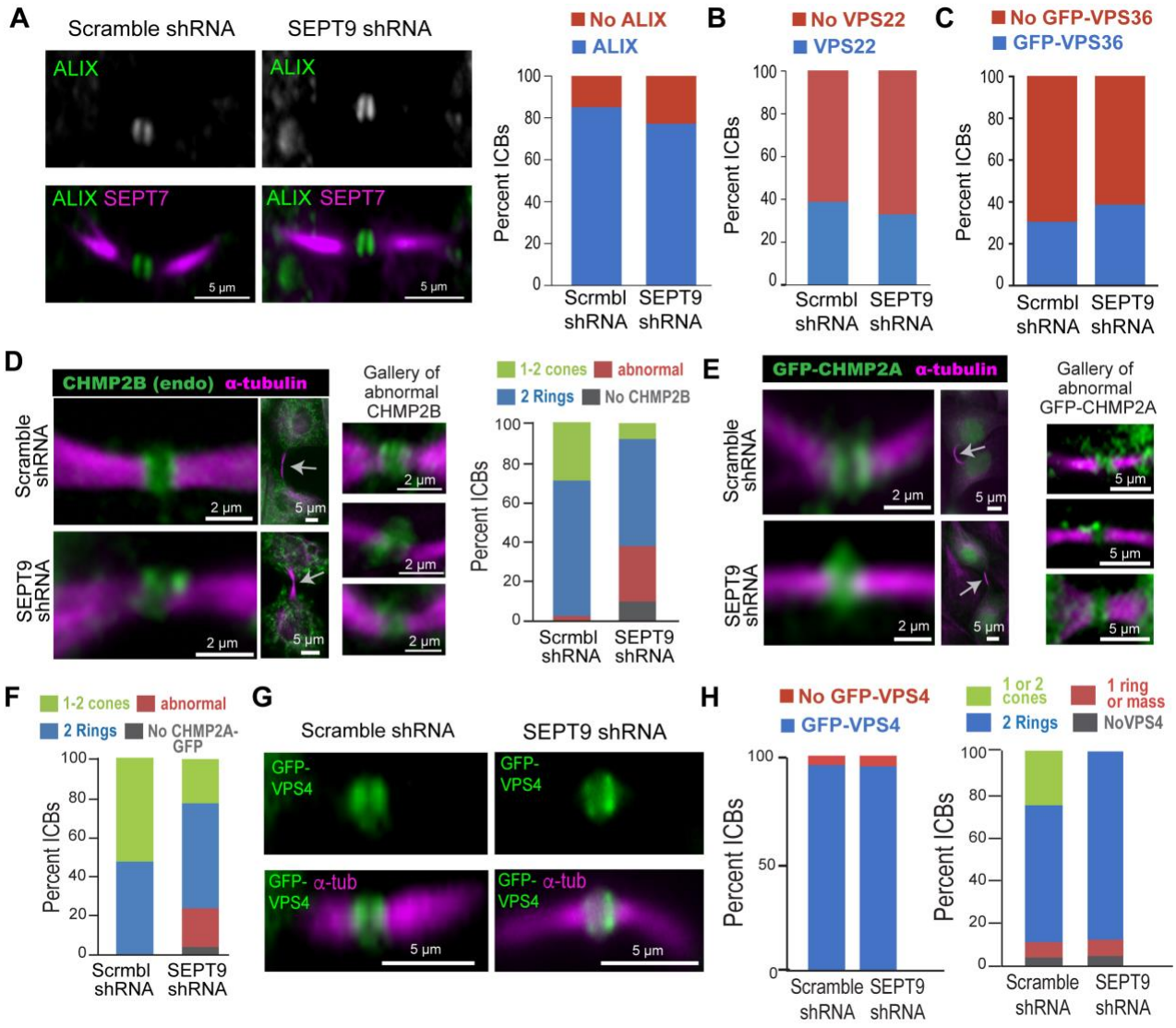

Figure S3. SEPT9 knock-down affects ESCRT-III (CHMP2B/CHMP2A) organization, but does not impact ALIX, VPS22, VSP36 and VPS4. Related to Figure 3.

(A) Images show ICBs of MDCK cells that express scramble and SEPT9 shRNAs after staining for endogenous ALIX and SEPT7. Bar graphs show the percentage of ICBs with ALIX in control (n = 46) and SEPT9 knock-down cells (n = 57).

(B-C) MDCK cells were transfected with a plasmid expressing scramble or SEPT9 shRNA and mCherry, and were stained for endogenous VPS22 (B) or imaged for GFP-VPS36 (C), which was transfected together with the shRNAs. Bar graphs show percentages of ICBs with VPS22 (B) in control (n = 52) and SEPT9-depleted cells (n = 46), and with GFP-VPS36 (C) in cells after treatment with scramble (n = 23) and SEPT9 shRNAs (n = 32).

(D) Representative images of ICBs (arrows) of MDCK cells stained for endogenous α-tubulin and CHMP2B after transfection with scramble and SEPT9 shRNAs that co-express mCherry (not shown). A gallery with examples of disorganized CHMP2B is shown. Graph shows percentage of ICBs without or with CHMP2B organized abnormally and as 2 rings or 1-2 cones in control (n = 49) and SEPT9-depleted cells (n = 45).

(E-F) Images (E) show the localization of GFP-CHMP2A in the ICBs (arrows) of MDCK cells, which were transfected with shRNAs and stained for α-tubulin. A gallery of disorganized GFP-CHMP2A phenotypes is shown. Bar graph (F) shows quantification of GFP-CHMP2A organization in control (n = 105) or SEPT9-depleted (n = 128) cells.

(G-H) Images show ICBs of MDCKs cells expressing GFP-VPS4 and shRNAs after staining with an antibody against α-tubulin. Bar graphs (H) show percentage of ICBs with and without GFP-VPS4 in control (n = 24) and SEPT9-depleted cells (n = 29), and percentage of ICBs with GFP-VPS4 organized as 1 ring or mass, 2 rings or 1-2 cones.

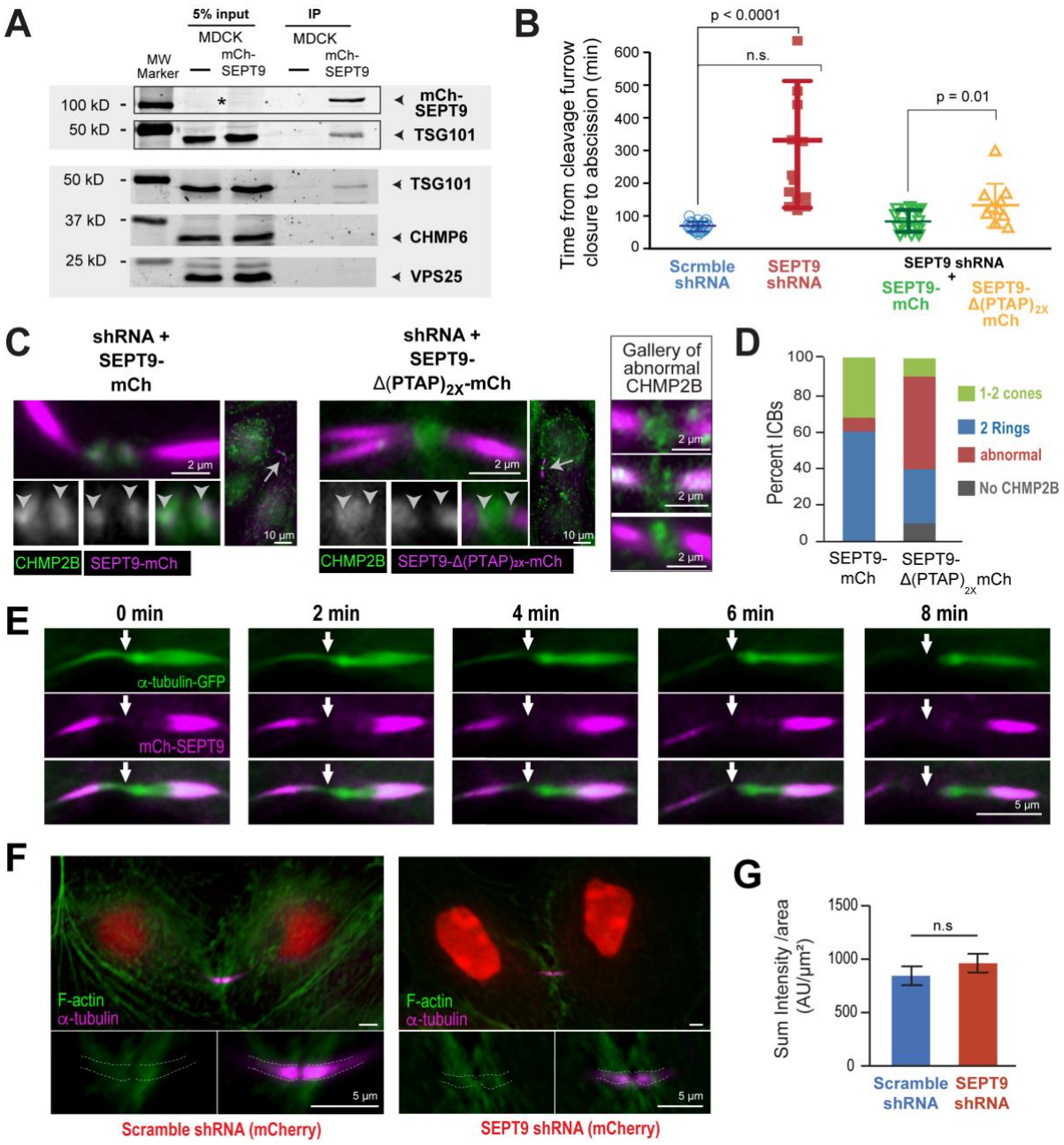

Figure S4. Abscission and CHMP2B organization are impacted by deletion of the TSG101-interacting PTAP motifs of SEPT9, which is not involved in MT severing and F-actin clearance. Related to Figures 4 and 1.

(A) Immunoprecipitations (IPs) were performed with RFP_Trap_A beads from extracts of untransfected MDCK cells and a stable MDCK cell line expressing mCherry-SEPT9 at sub-endogenous levels; note that mCherry-SEPT9 band is detectable upon IP and not seen in the 5% lysate input (asterisk). Western blots of SDS-PAGE gels from two different experiments are shown after incubation with antibodies against mCherry, TSG101, VPS25 and CHMP6.

(B) Plot shows the mean duration of abscission (± SD) in cells that completed abscission under 10 hours after transfection with scramble (n = 19) and SEPT9 shRNAs (n = 13), and upon transfection with plasmids co-expressing SEPT9 shRNAs and shRNA-resistant SEPT9-mCherry (n = 16) or SEPT9-Δ(PTAP)$_{2x}$-mCherry (n = 10).

(C-D) Representative images of ICBs (arrows) of MDCK cells stained for CHMP2B after transfection with plasmids that co-express SEPT9 shRNA and shRNA-resistant wild type SEPT9-mCherry or SEPT9-Δ(PTAP)$_{2x}$-mCherry (C). A gallery with examples of disorganized CHMP2B is shown. Arrowheads are fixed in location and point to overlap between CHMP2B and SEPT9 fluorescence. Bar graph (D) shows percentage of ICBs without or without CHMP2B organized abnormally and as 2 rings or 1-2 cones (n = 32-37 cells).

(E) Images show still frames from time-lapse movies of MDCK cells expressing GFP-α-tubulin and mCherry-SEPT9. Arrows point to the site of MT severing, which is devoid of mCherry-SEPT9.
(F-G) MDCK cells were transfected with plasmids expressing mCherry (red) and scramble or SEPT9 shRNAs, and were stained with phalloidin (F-actin) and an anti-α-tubulin antibody. Images (F) show the presence of F-actin in the midbody, which is outlined with a dashed line. Inset panel shows MTs in the cell body and the midbody of each cell is shown in higher magnification in separate panels. Bar graph (G) shows the sum intensity of F-actin per midbody surface area (± SEM) from cells with scramble (n = 32) and SEPT9 (n = 43) shRNAs. Note that MTs in the main cell body are not visible owing to the high brightness of midbody tubulin.

Name	Sequence
TSG101-VN (BifC)	
Forward	5’- AAAAAAGAATTCAATGGCGGTGTCG -3’
Reverse	5’- TTTTTTGTCGACGTAGAGGTCACT -3’
TSG101-VC (BifC)	
Forward	5’- AAAAAAGAATTCAAATGGCGGTGTCG -3’
Reverse	5’- TTTTTTCTCGAGTGTAGAGGTCACT -3’
SEPT9-VN (BifC)	
Forward	5’- AAAAAAAAGCTTATGAAGAAGTCT -3’
Reverse	5’- TTTTTTGTCGACCATCTCCGGGGC -3’
Canine SEPT9 shRNA targeting sequence	
Forward	5'-GATCCCCGACCGGCTGGTGAACGAGAAGTTTTCAAGAGAAACTTCTC GTTCACCAGCCGTCTTTTTA -3'
Reverse	5'-AGCTTAAAAAGACCGGCTGGTGAACGAGAAGTTTCTCTTGAAAACTTC TCGTTCACCAGCCG GTCGGG -3’
SEPT9 shRNA -resistant SEPT9 Δ$(PTAP)_{2x}$ -mCherry	
Forward	5'-GATGAGGACTCGGAGGACCGACTAGTAAATGAAAAGTTCCGGGAGAT GATCCC -3’
Reverse	5'-GGGATCATCTCCCGGAACTTTTCATTTACTAGTCGGTCCTCCGAGTCCT CATC -3'
GST-TSG101-UEV	
Forward	5’-AAAAAAAAGCTTATGGCGGTGTCGGAGAG-3’
Reverse	5’-TTTTTTCTCGAGTCAAGGACGAGAGAAGAC-3’

Table S1 - Sequence of primers used in present study. Related to STAR Methods.